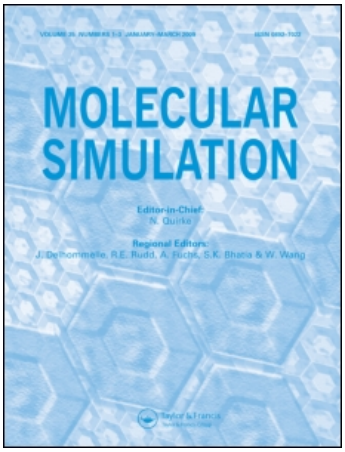

Molecular Simulation
Publication details, including instructions for authors and subscription information:
http://www.informaworld.com/smpp/title~content=t713644482

Prediction of protein conformation in water and on surfaces by Monte Carlo simulations using united-atom method

Abdulhakeem M. Al-Mekhnaqi[a]; Mohammed S. Mayeed[a]; Golam M. Newaz[ab]
[a] Department of Mechanical Engineering, Wayne State University, Detroit, MI, USA [b] Department of Biomedical Engineering, Wayne State University, Detroit, MI, USA

To cite this Article Al-Mekhnaqi, Abdulhakeem M. , Mayeed, Mohammed S. and Newaz, Golam M.(2009) 'Prediction of protein conformation in water and on surfaces by Monte Carlo simulations using united-atom method', Molecular Simulation, 35: 4, 292 — 300
To link to this Article: DOI: 10.1080/08927020802468364
URL: http://dx.doi.org/10.1080/08927020802468364

Molecular Simulation
Vol. 35, No. 4, April 2009, 292–300

Taylor & Francis
Taylor & Francis Group

Prediction of protein conformation in water and on surfaces by Monte Carlo simulations using united-atom method

Abdulhakeem M. Al-Mekhnaqi[a]*, Mohammed S. Mayeed[a] and Golam M. Newaz[ab]

[a]*Department of Mechanical Engineering, Wayne State University, Detroit, MI, USA;* [b]*Department of Biomedical Engineering, Wayne State University, Detroit, MI, USA*

(*Received 30 April 2008; final version received 10 September 2008*)

The united-atom method has been used to model an avian pancreatic polypeptide (APP) in water and the adsorption process of an albumin subdomain (AS) onto graphite surface to observe the capability of this lumped modelling approach to generate structures observed in protein data bank (PDB) and from atomistic modelling. The subdomain structure of a protein is simplified by the united-atom approximation where the side chains and peptide groups are represented by lumped spheres. The total potential energy of the adsorption process involves the interaction between these lumped spheres by means of virtual bond chain interaction and the interaction of the spheres with the graphite surface by means of Lennard-Jones potential. The protein/polypeptide structure has been perturbed by Monte Carlo with energy minimisation to obtain the global minimum. Results on the APP in water showed a near-to-experimental PDB conformation revealing the two α-helix structures of this small protein molecule with the root mean square deviation among carbon backbone atoms of 5.9 Å. Protein adsorption on biosurfaces has been made by modelling AS, which has 60 amino acids. The surface is graphite, which is characterised by its hydrophobicity. Graphite was chosen because of its widely used applications in certain implants that interact with blood. Our simulation results showed final conformation close to that obtained by atomistic modelling. It also proved that the whole pattern of intramolecular hydrogen bonds was distorted. The model also demonstrated the random conformation of the original α-helix secondary structures of AS consistent with experimental and atomistic results. While atomistic simulation works well for simulating individual small proteins, the united-atom model is more efficient when simulating macromolecular and multiple protein adsorption where time and limiting computer capacity are key factors.

Keywords: Monte Carlo simulation; local minimisation; united-atom method

Symbols

h	Planck's constant
k	Boltzmann's constant
n	refractive index
P	transition probability
r^{o}	the van der Waals radius
R_g	radius of gyration
S_{mn}	gyration tensor
T	absolute temperature
U_P	total pairwise protein bead–protein bead interaction
$U_{p_i p_j}$	peptide–peptide pairwise interaction
$U_{SC_i p_j}$	side chain–peptide pairwise interaction
$U_{SC_i SC_j}$	side chain–side chain pairwise interaction
U_t	total potential interaction
U_{tor}	torsional interaction potential
$\varepsilon(0)$	static or dielectric constants
ε_{ii}	standard energy parameter of the Lennard-Jones (LJ) potential between a protein bead and itself
ε_{ij}	standard energy parameter of the LJ potential between a bead and a carbon atom
ε_{jj}	standard energy parameter of the LJ potential between two carbon atoms in water
λ	principal axis
ν_e	medium absorption frequency

1. Introduction

The adsorption of proteins at the solid–liquid interface is the limiting factor in the long-term application of useful biomaterials. Long-term applications of contact lenses, blood-containing devices, fouling on kidney dialysis membranes are determined by the nature and amount of adsorbed proteins. Understanding the protein behaviour is important in the preparation and selection of right biocompatible materials for particular applications. Biomacromolecules such as proteins show a strong tendency to adsorb at liquid–solid interfaces because of van der Waals, ionic and polar interactions. In order to design and optimise these processes, accurate models of the adsorption mechanisms are needed.

Experimental studies of the activity and thermal stability of protein molecules by physical adsorption have shown that the adsorption process induces conformational changes and decreases the activity of the protein molecules compared with those in solution [1]. Other experimental methods like neutron reflection have been used to study the

*Corresponding author. Email: ai6408@wayne.edu

ISSN 0892-7022 print/ISSN 1029-0435 online

DOI: 10.1080/08927020802468364
http://www.informaworld.com

variation in the structure of adsorbed protein layers on solid surfaces with respect to bulk protein concentration and solution pH [2]. Surface-induced conformational changes in proteins have also been studied by using microfabricated cantilever sensors to measure the surface stress produced by protein adsorption onto metallic surfaces [3].

Because of the costly experimental analysis and of the expanding computational capabilities, researchers have been developing quantitative understanding of the mechanistic bases that drive proteins to accumulate at solid–liquid interfaces. With recent advances in computational capabilities, incorporation of atomic information for both proteins and surfaces into mechanistic models of protein adsorption has become attainable in some cases, but their application to macromolecules is still limited by computational resources. Atomistic models of proteins and polymer surfaces have been investigated in a few cases to calculate adsorption energies [4,5], and to investigate dynamic [6] and conformational [7] effects involving the adsorption of proteins onto polymer surfaces. The effects of the energetics of adsorption on different substrates and protein orientations, surface rearrangements and the kinetics of spreading have also been investigated [8,9]. Other works investigate the atomic details of the adsorbate–adsorbent surface interaction to address the effect of surface chemistry on the adsorption behaviour of proteins and understand the local adsorption features such as secondary structure change, characteristics of the different amino acid side groups and hydrogen bonds [10–12]. However, the problem of simulating entire protein molecules to be realistic remains demanding for extensive study. Consequently, a number of approaches have been applied in which the protein molecule is treated atomistically, but continuum approximations are made for the solvent and/or adsorbent [13]. Others have also described protein and polymer atomistically, using interatomic potentials designed to account for the presence of intervening water [14]. The solvation energy absent from such a description was added by a fragment method based on aqueous–organic transfer free energies of constituent amino acids [5,15]. This approach has been further extended to account for the presence of grafted polymer on the adsorbent substrate [16]. On the other hand, continuum or colloidal methods represent an alternative to atomistic approaches. However, colloidal methods treat a protein molecule as a rigid particle, which makes it almost impossible to account for conformational changes in the adsorption process.

Between the two extremes, molecular simulations based upon lattice and off-lattice models have been used in studying protein folding. Lattice models can capture some key features of a protein like chain connectivity and excluded-volume effect [17]. However, this kind of modelling is inefficient in predicting the helix secondary structure of protein molecules [18–21]. On the other hand, off-lattice Monte Carlo simulation [22,23] based on a coarse-grained model ignoring atomic details is an alternative approach to model the protein folding process with very high efficiency because of its capability to model α-helix, β-sheets and β-turns exhibited by real protein molecules. Thus, it allows finding the final conformational state of the protein whether in solution or adsorbed to the surface, which cannot be obtained by colloidal methods, and at the same time minimises the time which atomistic methods require. In this paper, the united-residue force field method [22,23] will be used to model avian pancreatic polypeptide (APP) in water and the adsorption process of an albumin subdomain (AS) onto graphite surface.

2. Theory

2.1 United-atom geometry

The first step for the simplification of the protein structure is to combine groups of atoms into single effective atoms, interaction centres [23]. The peptide group, which forms the backbone repeating unit, is simplified by combining the C′, N, O and H atoms into an effective atom. The side chain is simplified by treating it as a single effective atom. This simplified atom is located at the centroid of the atom positions of the side chain where the α-carbon atom is treated as a part of the side chain. In the united-atom model, the polypeptide chain is represented by a sequence of α-carbon atoms (C_α) with the side-chain atoms represented as a lumped mass (SC) attached to its associated C_α. The peptide group is also represented as a lumped mass (p) with its centre located between its associated α-carbons atoms, as shown in Figure 1.

In this model, C_α is considered as any atom initiating or terminating a peptide group including the terminal blocking groups such as acetyl or *N*-methylamide group. Because these blocking groups do not have any side chain attached to their C_α, these blocking groups are represented as a glycine residue. Since SC site represents all the atoms belonging to a real side chain and the corresponding

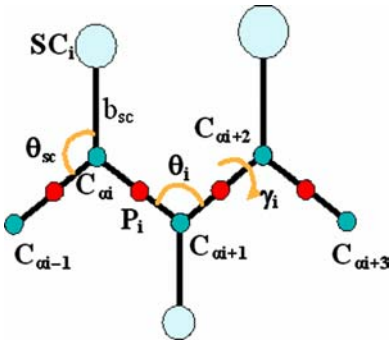

Figure 1. b_{sc} is the distance from SC to C_α, θ_{sc} is the planar angle defined by atoms SC_i—$C_{\alpha i}$—$C_{\alpha i-1}$ and γ_i is the virtual variable bond torsional angle about $C_{\alpha i+2}$ [23].

α-carbon atom, α-carbon atoms define the geometry of the backbone while the side chains and peptide groups are the only interaction sites in the energy evaluation. The atoms are collected together in the united-residue representation, when interaction energies are evaluated, where each p site represents the corresponding C′O—NH group. The polypeptide backbone geometry is defined by the distance between successive α-carbon atoms and the virtual bond angle θ that describes the plane C_α—C_α—C_α. The distance between a C_α site and the successive one is 3.8 Å, characteristic of a planar trans-peptide group. θ has a fixed value of 90°, which is an approximate value corresponding to the global maximum in the frequency distribution of virtual bond angles in protein crystal structures. The side-chain position is determined by a fixed bond length b_{sc} between the side chain and its corresponding C_α. This bond length varies from one residue to another, but is fixed for a specific residue. The orientation of the centroid of the side chain is determined by θ_{SC} and ϕ_{SC}. θ_{SC} is the angle formed by SC_i, $C_{\alpha i}$ and $C_{\alpha i-1}$, and ϕ_{SC} is the angle formed by SC_i—$C_{\alpha i}$—$C_{\alpha i-1}$ and $C_{\alpha i+1}$. Both θ_{SC} and ϕ_{SC} have fixed values for a particular residue but vary from one residue to another.

2.2 *Protein–protein interaction*

The complete energy function, ignoring Coulombic interactions on the charged residues, for the simplified chain is expressed as follows [23]:

$$U_P = \sum_i \sum_j U_{SC_iSC_j} + \sum_i \sum_j U_{SC_ip_j} + \sum_i \sum_j U_{p_ip_j} + \sum_i U_{tor}(\gamma_i), \quad (1)$$

where U_P is the total pairwise protein bead–protein bead interaction, $U_{SC_iSC_j}$ is the side chain–side chain pairwise interaction, $U_{SC_ip_j}$ is the side chain–peptide pairwise interaction, $U_{p_ip_j}$ is the peptide–peptide pairwise interaction and U_{tor} is the torsional interaction potential.

The term $U_{SC_iSC_j}$ is the average energy of interaction within an isolated pair of side chains i and j [23]:

$$U_{SC_iSC_j} = \left\{ \begin{array}{l} \varepsilon_{ij}\left[\left(\frac{r^o_{ij}}{r_{ij}}\right)^{12} - 2\left(\frac{r^o_{ij}}{r_{ij}}\right)^{6}\right] \\ -\varepsilon_{ij}\left(\frac{r^o_{ij}}{r_{ij}}\right)^{6} \end{array} \right\} \begin{array}{l} \text{for hydrophobic } (\varepsilon > 0) \\ \text{for hydrophilic } (\varepsilon < 0) \end{array} \quad (2)$$

with

$$r^o_{ij} = \frac{r^o_i + r^o_j}{2}, \quad (3)$$

where r^o_i is the van der Waals contact distance between SC_i beads, r^o_j is the van der Waals contact distance between SC_j beads and r^o_{ij} is the van der Waals contact distance between SC_i and SC_j.

The van der Waals radii are taken from set C of Levitt [24]. The ε's are calculated from the inter-residue contact energies of Miyazawa and Jernigan [25].

When residues i and j are not in contact, the average SC–p interactions cannot be neglected and a simple excluded-volume potential is used [23]

$$U_{SC_ip_j} = \varepsilon_{SCp}\left(\frac{r^o_{SCp}}{r_{ij}}\right)^6. \quad (4)$$

The process of calculating the p–p interactions is based on averaging the dipole interactions between peptide groups and given by [23]

$$\overline{U}_{ij} = \frac{A_{p_ip_j}}{r^3_{ij}}(\cos\alpha_{ij} - 3\cos\beta_{ij}\cos\gamma_{ij}) - \frac{B_{p_ip_j}}{r^6_{ij}}[4 + (\cos\alpha_{ij} - 3\cos\beta_{ij}\cos\gamma_{ij})^2 - 3(\cos^2\beta_{ij} + \cos^2\gamma_{ij})] + \varepsilon_{p_ip_j}\left[\left(\frac{r^o_{p_ip_j}}{r_{ij}}\right)^{12} - 2\left(\frac{r^o_{p_ip_j}}{r_{ij}}\right)^{6}\right]. \quad (5)$$

The angles α_{ij} is the angle between $C\alpha_i$—$C\alpha_{i+1}$ and $C\alpha_j$—$C\alpha_{j+1}$, β_{ij} is the angle between $C\alpha_i$—$C\alpha_{i+1}$ and r_{ij}, and γ_{ij} is the angle between $C\alpha_j$—$C\alpha_{j+1}$ and r_{ij}. Empirical conformational energy program for peptides (ECEPP/2) is then [23] used to average the values of $A_{p_ip_j}$, $B_{p_ip_j}$ and ε_{ij}.

The last term in Equation (1), the torsional energy is given by the Fourier series [23]

$$U^{XY}_{tor}(\gamma_i) = a_o + \sum_{k=1}^{6}(a_k\cos k\gamma_i + b_k\sin k\gamma_i), \quad (6)$$

where the Fourier coefficients are reported in [23]. In this model, the alanine residue is assumed to represent all the L-amino acid residues except proline, which has a different pattern of local interactions, and glycine, which is also a special case because it is not chiral. This representation leads to further approximation of the united-atom model.

2.3 *Protein–surface interaction and geometry*

The total protein–surface intermolecular pair potential is obtained by summing the attractive and repulsive potentials. The best known of these is the LJ or 6-12 potential

$$U_{ps} = \sum_i \sum_j \varepsilon_{ij}\left[\left(\frac{r^o_{ij}}{r_{ij}}\right)^{12} - 2\left(\frac{r^o_{ij}}{r_{ij}}\right)^{6}\right], \quad (7)$$

where U_{ps} is the sum of all the interactions between protein

beads and their effective carbon atoms, ε_{ij} is the standard energy parameter of the LJ potential and r_{ij} is the distance between the centres of the bead and the carbon atom. To calculate the standard energy parameter of the LJ potential of a protein bead and the corresponding graphite surface atom, the Lorentz–Berthelot combining rules are used, where

$$\varepsilon_{ij} = \sqrt{\varepsilon_{ii}\varepsilon_{jj}} \text{ and } r_{ij}^{\text{o}} = \frac{r_{ii}^{\text{o}} + r_{jj}^{\text{o}}}{2}, \tag{8}$$

where ε_{ii} is the standard energy parameter of the LJ potential between a protein bead and itself, ε_{jj} is the standard energy parameter of the LJ potential between two carbon atoms in water, r_{ii}^{o} is the van der Waals contact distance between two protein beads, r_{jj}^{o} is the van der Waals contact distance between two carbon atoms and r_{ij}^{o} is the van der Waals contact distance between a protein bead and a carbon atom. While ε_{ii} values are determined experimentally, ε_{jj} values need to be evaluated.

The theory of McLachlan can be applied to evaluate the interactions of molecules or small particles in a medium. The total van der Waals interaction free energy of two identical molecules or small particle 1 in medium 3 can be expressed as [26]

$$w(r) \approx \left[3kT\left(\frac{\varepsilon_1(0)-\varepsilon_3(0)}{\varepsilon_1(0)+2\varepsilon_3(0)}\right)^2 + \frac{\sqrt{3}h\nu_{\text{e}}}{4}\frac{(n_1^2-n_3^2)^2}{(n_1^2+2n_3^2)^{3/2}}\right]\frac{a_1^6}{r^6}, \tag{9}$$

where k is Boltzmann's constant, h is Planck's constant, T is the absolute temperature, ν_{e} is the medium absorption frequency, $\varepsilon_1(0)$, and $\varepsilon_3(0)$ are the static or dielectric constants of the particle 1 and medium 3, respectively, and n_1 and n_3 are the refractive indices of the particle and medium, respectively. Thus, the standard energy parameter of the LJ potential between two carbon atoms in solvent can be expressed as

$$\varepsilon_{ii} = \frac{1}{2}\left[3kT\left(\frac{\varepsilon_1(0)-\varepsilon_3(0)}{\varepsilon_1(0)+2\varepsilon_3(0)}\right)^2 + \frac{\sqrt{3}h\nu_{\text{e}}}{4}\frac{(n_1^2-n_3^2)^2}{(n_1^2+2n_3^2)^{3/2}}\right]. \tag{10}$$

Once ε_{ii} is determined, ε_{ij} can be calculated using Equation (8) and the total potential interaction can be calculated as

$$U_{\text{t}} = U_{\text{ps}} + U_{\text{p}}. \tag{11}$$

The graphite surface is chosen as a model biomaterial because of its relative simplicity and rigidity, so that it can be treated as a fully rigid body. The flat sheets of carbon atoms are bonded into hexagonal structures. These exist in layers that are not covalently connected to the surrounding layers. Instead, different layers are connected together by the weak van der Waals forces.

In the simulation, only two carbon layers are used, no additional planes being necessary based on literature results [27], using the interaction up to six layers. Since the graphite surface is infinite, it is crucial for the software to be effective by assigning the interaction of the bead with only those surface atoms that are within a convenient cut-off range, as shown in Figure 2. The code is used to evaluate the total potential interaction between a bead and the surface. It starts the calculation by assuming two atoms on the sides. The length of the side is incremented to a final value of 73 Å for all hydrophobic (Figure 3) and hydrophilic (Figure 4) amino acid residues. The potential interaction with 73 Å along a side was representative of the value of infinite number of graphite carbon atoms. Choosing a cut-off number of 23 Å along a side was enough to give accurate potential calculations. At contact with the graphite surface, both trp, among the hydrophobic set, and arg, among the hydrophilic set, suffered the most approximation errors. Defining the error % as

$$\text{error}\,\% = \left|\frac{u_{73} - u_{23}}{u_{73}}\right| \times 100\%, \tag{12}$$

where u_{73} and u_{23} denote the potential interaction with 73 and 23 Å along a side. The error percentages for trp and arg were 1.97 and 1.87%, respectively.

2.4 Energy minimisation

Figure 5 shows the flow chart of the global optimisation of the interaction function. The algorithm uses Monte Carlo with energy minimisation (MCM) scheme to generate a Markov walk on all discrete energy minima, with Boltzmann transition probabilities using Metropolis algorithm. MCM is the engine that repeatedly generates a Markov chain of states that have Boltzmann probability distribution, in order to simulate real systems. For a Markov process to achieve the Boltzmann probability distribution, it should satisfy the conditions of ergodicity and detailed balance. The condition of ergodicity is the requirement that it should be possible for a Markov process to reach any state of the system from any other state. Detailed balance states that at equilibrium the ratio of the transition probabilities from state a to b should be equal to the ratio of their probabilities. The well-known Metropolis algorithm is as follows:

$$P(\text{a} \rightarrow \text{b}) = \begin{cases} 1 & \text{if } E_{\text{b}} \le E_{\text{a}} \\ \text{e}^{-\beta(E_{\text{b}}-E_{\text{a}})} & \text{if } E_{\text{b}} > E_{\text{a}} \end{cases}, \tag{13}$$

where $P(\text{a} \rightarrow \text{b})$ is the transition probability from state a to b, β is equal to $1/(kT)$, E_{b} is the energy of state b and E_{a} is the energy of state a.

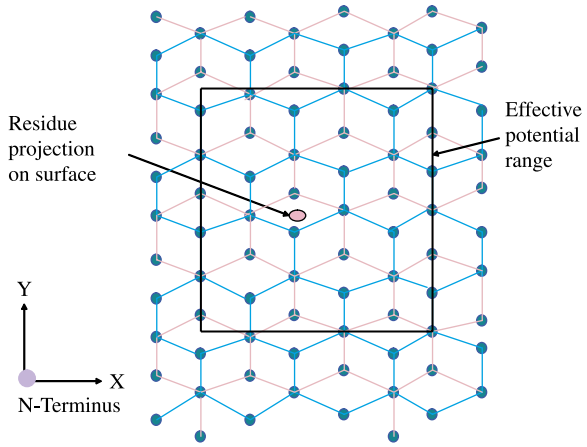

Figure 2. The number of effective interacting graphite atoms with a protein bead.

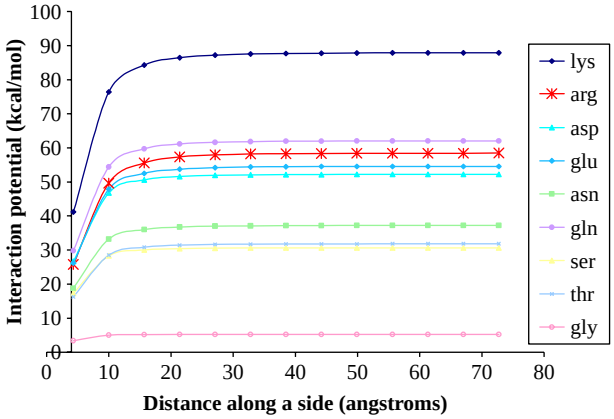

Figure 4. Potential interaction for hydrophilic residues *vs.* the number of atoms along a side.

If $E_b \leq E_a$, the algorithm chooses state b to be the new state; if $E_b > E_a$, the algorithm chooses a random number R uniformly between 0 and 1. If $P(a \rightarrow b) > R$, b becomes the new state; otherwise, the system stays at state a.

For the algorithm to be more efficient, the chosen states are to be local minima through the space conformation. Direct search scheme [28] is employed to locally minimise the interaction energies as shown in the flow chart of Figure 6. The direct search operates in the following manner.

Initial values of all the elements as well as an initial incremental change must be provided. To initiate an exploratory search, the objective function, which is the sum of all the interactions energy, U_t is evaluated at a base point. Then γ_i is changed by a positive incremental amount Δ. If U_t is reduced, $\gamma_i + \Delta$ is adopted as the new element in the vector of the dihedral angles $\boldsymbol{\gamma}$. If the increment fails to reduce U_t, γ_i is changed by $-\Delta$ and the value of U_t is checked again. If the value of U_t is not improved by both the increments, γ_i is left unchanged. The successful increments define a path that represents a successful direction for the search along which subsequent pattern search is made. This search is called exploratory search type I. After this, the exploratory search type II is performed. If U_t is not decreased after type II exploratory search, the pattern search is said to fail, and a new type I exploratory search is made in order to give a new successful direction. If type I fails to give a new successful direction, Δ is reduced gradually, until either a new successful direction can be defined or Δ becomes smaller than some prescribed value, at which the search ends and the final value of U_t is said to be a local minimum.

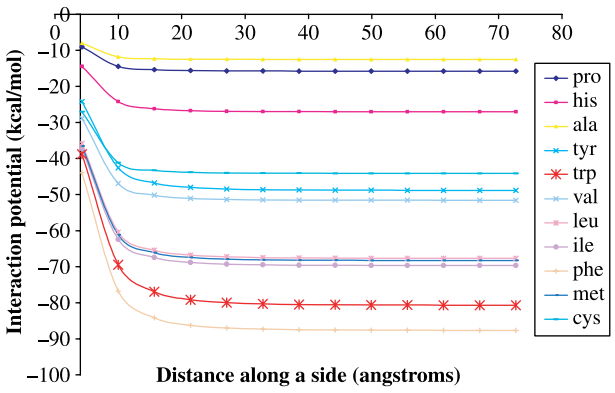

Figure 3. Potential interaction for hydrophobic residues *vs.* the number of atoms along a side.

3. Results and discussion

In the analysis, MCM starts with the fully extended conformation as its initial local minimum. Only one random dihedral angle γ is given a random value between $-180°$ and $180°$. This conformation is then subjected to conventional energy minimisation using direct search scheme to obtain the nearest local minimum conformation. Another dihedral angle γ is randomly chosen and again given a random value between $-180°$ and $180°$ followed by conventional energy minimisation to reach the nearest local minimum for a finite number of random sampling steps. Metropolis criterion is used to decide which conformation is to be kept. This procedure continues until a preassigned number of perturbations are reached. This preassigned number is determined by first assuming some small iteration limit. Then, this number is applied for two runs. Next, the total energy difference in the final conformations of the two runs is calculated. The iteration limit is increased until the difference in the total energies of the final conformations reaches to an acceptable value.

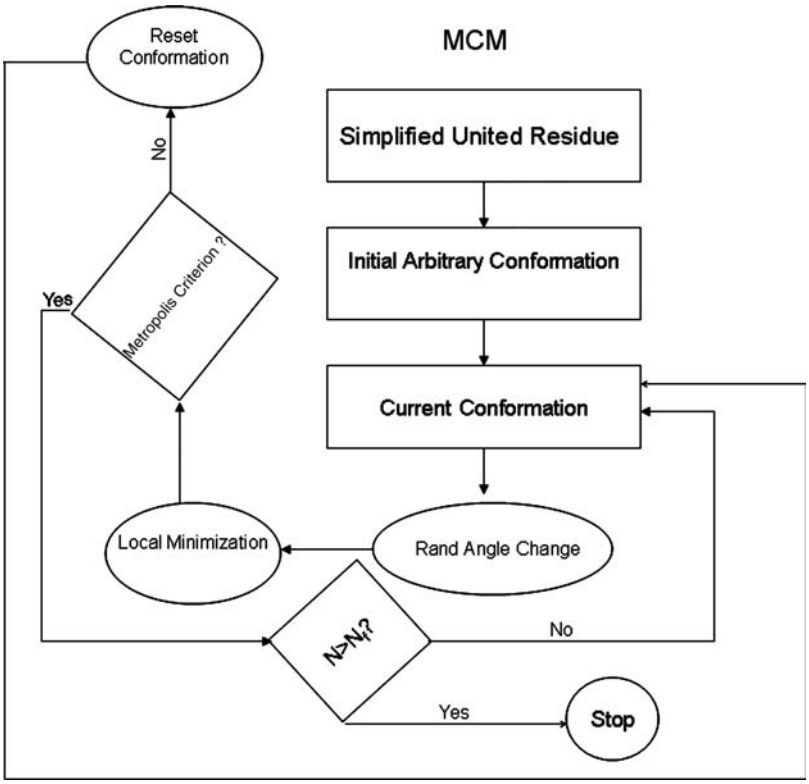

Figure 5. Flow chart of MCM for determining the native structure of protein.

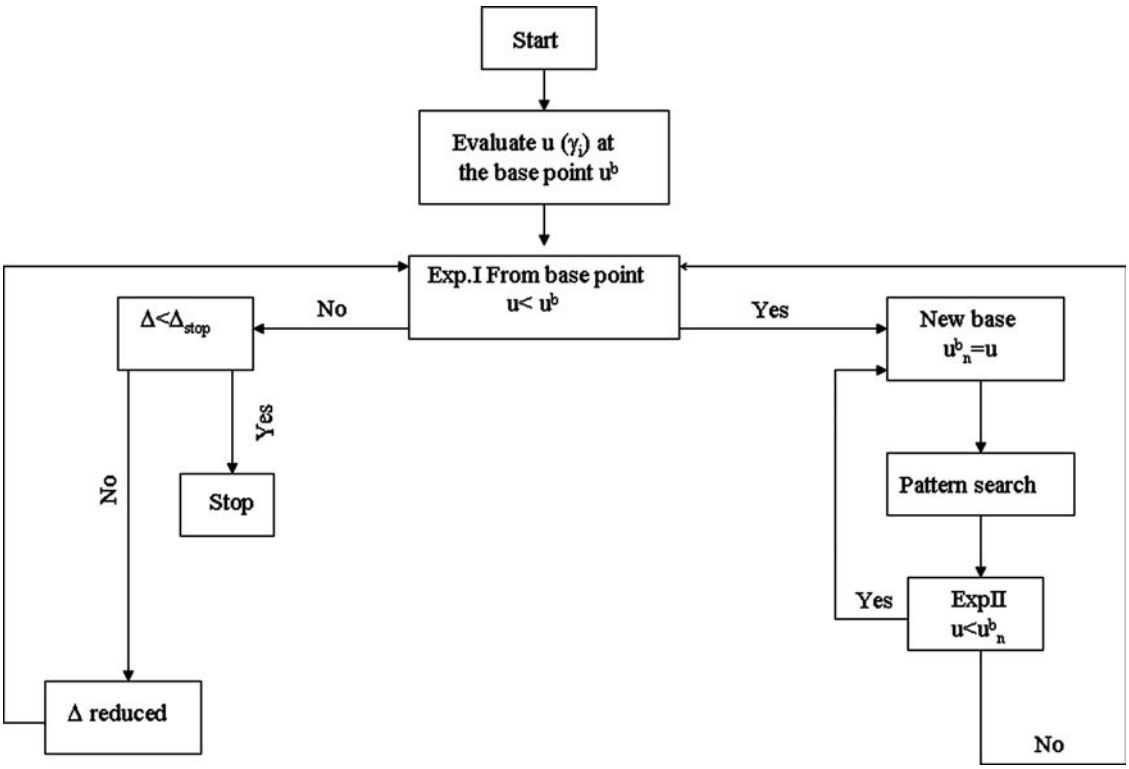

Figure 6. Local minimisation flow chart.

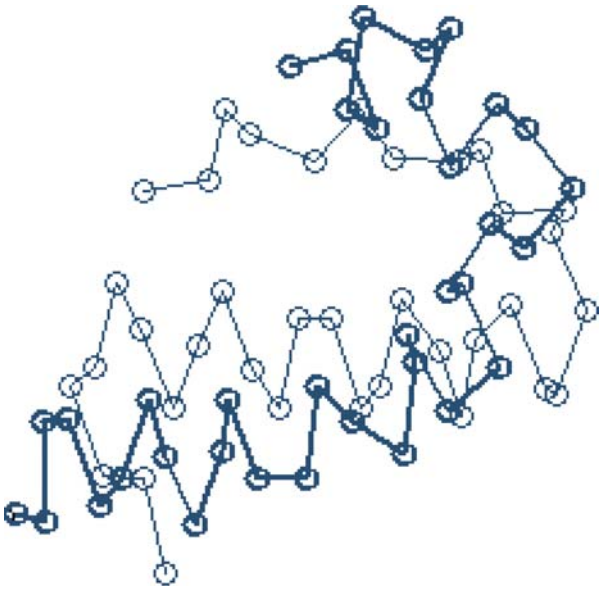

Figure 7. APP native structure in water by the computational model superimposed to that from the PDB giving an RMSD of 5.94 Å.

3.1 APP in solution

Analysis has been made to determine the native state of APP in water. APP is a small 36-residue protein structure, determined by Glover et al. [29] at a resolution of 0.98 Å. The structure consists of an α-helix running from residues 1 to 8, packed against the face of an α-helix that extends from residues 13 to 31. An MCM of 2000 cycles has been necessary to determine the near-to-native structure of APP in water with a total potential of −139 kcal/mol. The computational result shows close-to-native conformation of APP in water with the first helix containing amino acids of 1–10 and the second helix containing amino acids of 13–32. In order to quantify the conformation obtained by the united-atom method in comparison with that given by Glover [29], the root mean square deviation (RMSD) is to be calculated

$$\mathrm{RMSD} = \sqrt{\frac{\sum_{i=1}^{n} (d_i^{\mathrm{a}} - d_i^{\mathrm{e}})^2}{n}}, \tag{14}$$

where n is the total number of amino acid residues, d_i^{a} is the distance between the ith amino acid given by the computational model and the origin, and d_i^{e} is the distance between the ith amino acid given by the protein data bank (PDB) and the origin. In order to obtain the best 3D superposition, a series of local rigid rotational and translational movements for computationally obtained APP structure has been necessary. Several phases have been observed and the last phase (Figure 7) gives an RMSD value of 5.94 Å, after which it has not decreased any further.

3.2 AS adsorption onto graphite

Adsorption of AS on a graphite surface was modelled to determine the ultimate state of the adsorbed polypeptide. AS is a small fragment of albumin comprising the amino acids from Ser5 to Lys64, totalling to 60 residues [27]. The surface is of graphite characterised by its hydrophobic characteristics, and its relative simplicity and rigidity. The united-atom MCM run started with the completely extended chain, i.e. all dihedral angles γ set at 180°. A total number of 2500 MCM cycles were necessary to generate the final conformation, as shown in Figure 8(a), having a total potential interaction of −256.84 kcal/mol. The conformation of AS obtained by the united-atom model looks similar to that obtained by atomistic modelling [27], which is shown in Figure 8(b). This structure shows random portions (broken helices) of AS consistent with that of the atomistic simulation [27], which

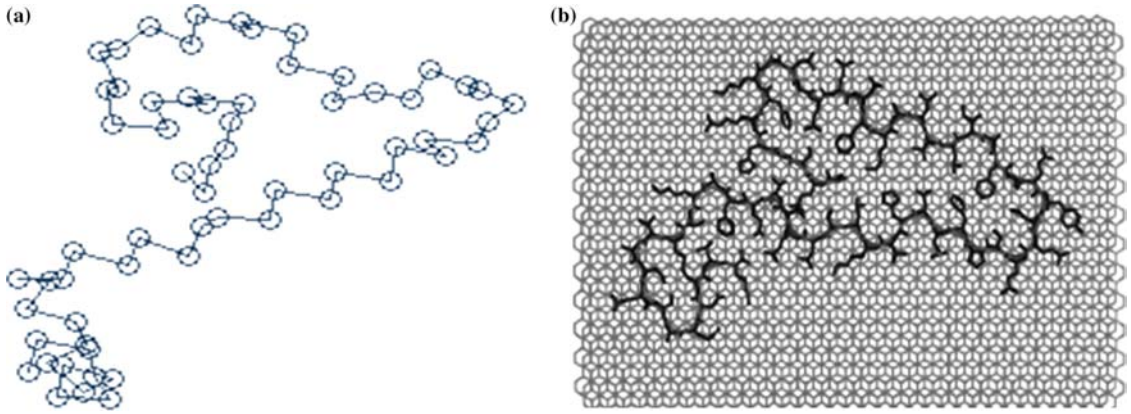

Figure 8. (a) MCM result of AS conformation during adsorption on a graphite surface at a total interaction potential of −256.84 kcal/mol. (b) Atomistic simulation result of AS adsorbed onto a graphite surface by Raffaini and Ganazzoli [27].

were originally α-helix structures at their native conformational state in the mother albumin protein.

The gyration tensor for a collection of particles is given by

$$S_{mn} = \frac{1}{N}\sum_{i=1}^{n} r_m^{(i)} r_n^{(i)}, \tag{15}$$

where N is the number of particles and $r_m^{(i)}$ is the mth Cartesian coordinate of the position vector $r^{(i)}$ of the ith particle.

We can calculate the values of the principal axes from the diagonal matrix of the gyration tensor of AS and the radius of gyration R_g is given by

$$R_g = \sqrt{\lambda_1^2 + \lambda_2^2 + \lambda_3^2}. \tag{16}$$

The results are consistent with the experimental observation that soft proteins, such as albumins, undergo large conformational changes on hydrophobic surfaces. The radius of gyration of the final adsorbed AS structure, as shown in Figure 8(b), with the origin of the Cartesian coordinates at the centre of mass, is 22.4 Å close to that given by the atomistic modelling, which is 21.5 Å. The values of λ_1, λ_2 and λ_3 by the united-atom model are, respectively, 18.4, 11.8 and 4.8 Å, compared with 19.3, 9.3 and 1.0 Å in the atomistic modelling. In particular, λ_3, perpendicular to the graphite surface, becomes small compared with the parallel axes λ_1 and λ_2 in both the united-atom and atomistic modellings. However, in the united-atom modelling, λ_3 remains larger compared with that observed in the atomistic modelling. We think this discrepancy occurs because the final conformation does not correspond to a true monolayer of amino acids as can be observed from the self-overlap of backbone, as shown in Figure 8(b).

4. Conclusions

The united-atom model can generate the native state of APP in water showing quantitative comparison with that of the PDB. For AS adsorption to a graphite surface, the united-atom results suggest that the denaturation is sufficiently complete and the molecule unfolds into loose random structures on the surface similar to the results observed by the experiment. The conformational changes on the hydrophobic surface were quantified in terms of the radius of gyration of 22.4 Å compared with 21.5 Å given by the atomistic modelling. The parallel principal axes of 18.4 and 11.8 Å came close enough to those given by the atomistic modelling of 19.3 and 9.3 Å, respectively. However, simplification has always its price in reduced precision, and nevertheless there is always a trade-off between precision and computational power. With the current state-of-the-art computational facilities to model a device design aspect that needs protein modelling, lumped approach like the united-atom model is an absolute necessity. The united-atom potential field must be tested on a larger number of known protein structures in solutions and on surfaces in order to assess the versatility of the method. The application of the united-atom model using MCM presented here is the first step towards the development of a realistic and more detailed understanding of how the solution and surface properties affect the adsorption behaviour of protein molecules in a multibody system. Future studies are aimed at using this simplified protein model to study the effects of surface roughness, chemical composition, surface charges and solution pH on the secondary and tertiary structure formation, and to study the competition between protein folding and aggregation in multiprotein environments. By sacrificing some of the physical details present in the detailed atomistic protein models, the united-atom model may allow the simulations of significantly larger and more complicated protein systems within more realistic time frames.

References

[1] T. Zoungrana and W. Norde, *Thermal stability and enzymatic activity of α-chymotrypsin adsorbed on polystyrene surfaces*, Colloids Surf. B: Biointerfaces 9 (1997), pp. 157–167.

[2] J. Lu, T. Su, P. Thirtle, R. Thomas, A. Rennie, and R. Cubitt, *The denaturation of lysozyme layers adsorbed at the hydrophobic solid/liquid surface studied by neutron reflection*, J. Colloid Interf. Sci. 206 (1998), pp. 212–223.

[3] A. Moulin, S. O'Shea, R. Badley, P. Doyle, and M. Welland, *Measuring surface-induced conformational changes in proteins*, Langmuir 15 (1999), pp. 8776–8779.

[4] D. Lu and K. Park, *Protein adsorption on polymer surfaces: Calculation of adsorption energies*, J. Biomater. Sci. Polym. Edn. 1 (1990), pp. 243–260.

[5] S. Lee and K. Park, *Protein interaction with surfaces: Separation distance-dependent interaction energies*, J. Vac. Sci. Techhnol. A 12 (1994), pp. 2949–2959.

[6] K. Lim and J. Herron, *Molecular simulation of protein–PEG interaction*, in *Poly(ethylene Glycol) Chemistry: Biotechnical and Biomedical Applications*, J. Harris, ed., Plenum Press, New York, 1992, pp. 29–55.

[7] D. Tobias, W. Mar, J. Blasie, and M. Klein, *Molecular dynamics simulations of a protein on hydrophobic and hydrophilic surfaces*, Biophys. J. 71 (1996), pp. 2933–2941.

[8] F. Ganazzoli and G. Raffaini, *Computer simulation of polypeptide adsorption on model biomaterials*, Phys. Chem. Chem. Phys. 7 (2005), pp. 3651–3663.

[9] G. Raffaini and F. Ganazzoli, *Understanding the performance of biomaterials through molecular modeling: Crossing the bridge between their intrinsic properties and the surface adsorption of proteins*, Macromol. Biosci. 7 (2007), pp. 552–556.

[10] M. Agashe, V. Raut, S. Stuart, and R. Latour, *Molecular simulation to characterize the adsorption behavior of a fibrinogen γ-chain fragment*, Langmuir 21 (2005), pp. 1103–1117.

[11] A. Cormack, R. Lewis, and A. Goldstein, *Computer simulation of protein adsorption to a material surface in aqueous solution: Biomaterials modeling of a ternary system*, J. Phys. Chem. B 108 (2004), pp. 20408–20418.

[12] J. Shen, T. Wu, Q. Wang, and H. Pan, *Molecular simulation of protein adsorption and desorption on hydroxyapatite surfaces*, Biomaterials 29 (2008), pp. 513–532.

[13] V. Noinville, C. Vidal-Madjar, and B. Sebille, *Modeling of protein adsorption on polymer surfaces. computation of adsorption potential*, J. Phys. Chem. 99 (1995), pp. 1516–1522.
[14] S. Weiner, P. Kollman, D. Case, U. Singh, C. Ghio, G. Algona, S. Profeta, and P. Weiner, *A new force field for molecular mechanical simulation of nucleic acids and proteins*, J. Am. Chem. Soc. 106 (1984), pp. 765–784.
[15] D. Lu, S. Lee, and K. Park, *Calculations of solvation interaction energies for protein adsorption on polymer surfaces*, J. Biomater. Sci. Polym. Edn. 3 (1991), pp. 127–147.
[16] I. Szleifer, *Protein adsorption on surfaces with grafted polymers: A theoretical approach*, Biophys. J. 72 (1997), pp. 595–612.
[17] K. Lau and K. Dill, *A lattice statistical mechanics model of the conformational and sequence spaces of proteins*, Macromolecules 22 (1989), pp. 3986–3997.
[18] J. Skolnick and A. Kolinski, *Simulations of the folding of a globular protein*, Science 250 (1990), pp. 1121–1125.
[19] A. Sikorski, A. Kolinski, and J. Skolnick, *Computer simulations of de novo designed helical proteins*, Biophys. J. 75 (1998), pp. 92–105.
[20] B. Ilkowski, J. Skolnick, and A. Kolinski, *Helix-coil and beta sheet-coil transitions in a simplified, yet realistic protein model*, Macromol. Theory Simul. 9 (2000), pp. 523–533.
[21] C. Chen, *Lattice model of transmembrane polypeptide folding*, Phys. Rev. E 63 (2000), pp. 0109011–0109014.
[22] A. Liwo, M. Pincus, R. Wawak, S. Rackovsky, and H. Scheraga, *Calculation of protein backbone geometry from α-carbon coordinates based on peptide-group dipole alignment*, Protein Sci. 2 (1993), pp. 1697–1714.
[23] A. Liwo, M. Pincus, R. Wawak, S. Rackovsky, and H. Scheraga, *Prediction of protein conformation on the basis of a search for compact structures: Test on avian pancreatic polypeptide*, Protein Sci. 2 (1993), pp. 1715–1731.
[24] M. Levitt, *A simplified representation of protein conformations for rapid simulation of protein folding*, J. Mol. Biol. 104 (1976), pp. 59–107.
[25] S. Miyazawa and R. Jernigan, *Estimation of effective interresidue contact energies from protein crystal structures: Quasi-chemical approximation*, Macromolecules 18 (1985), pp. 534–552.
[26] J. Israelachvili, *Intermolecular and Surface Forces: With Applications to Colloidal and Biological Systems*, Academic Press, London, 1985.
[27] G. Raffaini and F. Ganazzoli, *Simulation study of the interaction of some albumin subdomains with a flat graphite surface*, Langmuir 19 (2003), pp. 3403–3412.
[28] M. David, *Applied Nonlinear Programming*, McGraw Hill, New York, 1972.
[29] I. Glover, I. Haneef, J. Pitts, S. Wood, D. Moss, I. Tickle, and T. Blundell, *Conformational flexibility in a small globular hotmone: X-ray analysis of avian pancreatic polypeptide at 0.98-A resolution*, Biopolymers 22 (1983), pp. 293–304.